Reducing Coil Characteristics Deterioration by Using Insulated Rebar Testbody in Dynamic Wireless Power Transfer

Kaito Matsuo
Faculty of Science and Engineering
Tokyo University of Science
Noda, Japan
7319121@ed.tus.ac.jp

Takehiro Imura
Faculty of Science and Engineering
Tokyo University of Science
Noda, Japan

Yoichi Hori
Faculty of Science and Engineering
Tokyo University of Science
Noda, Japan

Megumu Kunigo
Technical Development Department
GAEART Co., Ltd.
Tokyo, Japan

Shun Shimizu
Technical Research and Development Division
Kumagai Gumi Co.,Ltd.
Tokyo, Japan

Shunsuke Maki
Technical Research and Development Division
Kumagai Gumi Co.,Ltd.
Tokyo, Japan

***Abstract*— In dynamic wireless power transfer (DWPT), it is essential to embed the power transmission coils in the road. Previous studies have reported that the properties deteriorate during embedment in reinforced concrete pavements because of rebar and concrete. In this paper, a reinforced concrete testbody was used to simulate the embedment of the coils in the pavement and to measure the properties of the coils because of the embedment. We propose a method to reduce the deterioration of properties by changing the rebar used in the testbody to be insulated rebar. As a result of measurements with a vector network analyzer (VNA), the use of insulated rebar reduced the *Q-value* of the coil by about 30 % compared to that of normal rebar. Furthermore, a transmission efficiency of 93.2 % was obtained at an air gap of 170 mm.**

Keywords—Wireless Power Transfer, Dynamic Wireless Power Transfer, Reinforced Concrete, Coil embedment

I. INTRODUCTION

The replacement of gasoline and diesel vehicles with electric vehicles (EVs) is gaining importance around the world to achieve carbon neutral. However, EVs have a short cruising range, lack of charging infrastructure, and other issues that have slowed the spread of EVs. To solve these problems is wireless DWPT (Dynamic Wireless Power Transfer), which is being actively researched [1]-[8].

For the practical application of DWPT, it is essential that the transmission coils be embedded in the pavement. However, it has been reported that embedding the coils degrades their properties because of the surrounding environment, such as rebar, concrete, and asphalt [9]-[18]. Furthermore, it has been reported that not only do coil characteristics deteriorate, but transmission efficiency also decreases. This paper focuses on embedment with respect to reinforced concrete pavements and proposes embedment in reinforced concrete pavements with insulated steel bars as a method of reducing the deterioration of the properties of coil embedment. The use of insulated rebar is expected to have the effect of reducing the effects of the rebar itself, as well as eddy current losses and resonance misalignment when high power is applied.

In Japan, asphalt pavements account for about 95 %, in the US and EU about 80 %, and in Korea about 40 %, with reinforced concrete pavements accounting for the remaining percentage. Reinforced concrete pavements account for only a small percentage in Japan. However, in Japan, rural trunk roads, metropolitan expressways, bridges, and tunnels, which are important for logistics, are reinforced concrete pavements, and for practical use, it is essential to study not only embedding in asphalt pavements, but also in reinforced concrete pavements. Furthermore, compared to asphalt pavements, reinforced

concrete pavements have recently received renewed attention due to their durability, water resistance, seismic resistance, and lower maintenance and repair costs, and the percentage of implementation is likely to increase in the future.

Therefore, this paper examines methods of reducing characteristic deterioration and improving transmission efficiency by using a testbody with insulated steel bars to simulate embedment.

II. Reinfoced Concrete Testbody

The reinforced concrete test bodies used in this measurement are shown below. The dimensions of the testbody created are 2000 x 1180 x 295 mm, with a box-cut portion 2000 x 980 x 120 mm on top of the testbody. The area where the coils of the precast RC slab will be buried during the actual embedment is the box removal area. The distance from the rebar to the bottom of the box-cutter is 30 mm. In addition, two types of rebar were made for the test body: normal rebar and insulated rebar. Concrete blocks of 160 x 160 x 20 mm, 160 x 160 x 40 mm, and 160 x 160 x 60 mm were also made to simulate embedment. Fig. 1 shows a schematic drawing of the test body, and Fig. 2 shows the actual test bodies and concrete blocks. Furthermore, a schematic diagram of the experiment is shown in Fig. 3, and a complete diagram of the practical application is shown in Fig. 4.

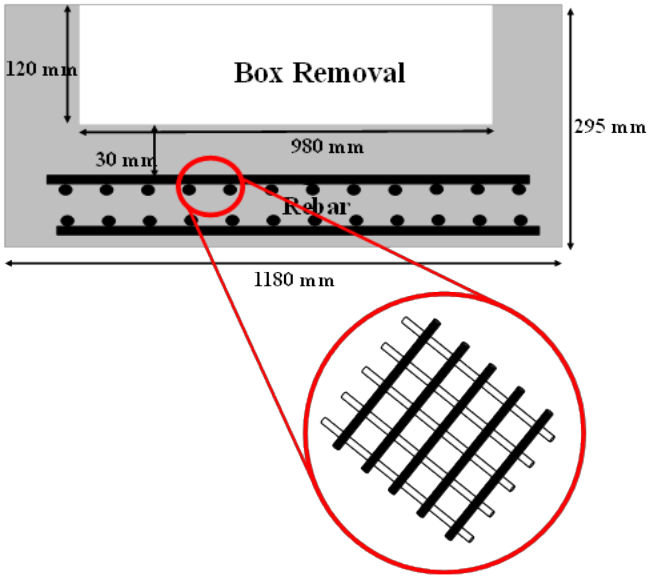

Fig. 1. Schematic diagram of the test body.

Fig. 2. Test Body (Right) and Concrete Block (Left).

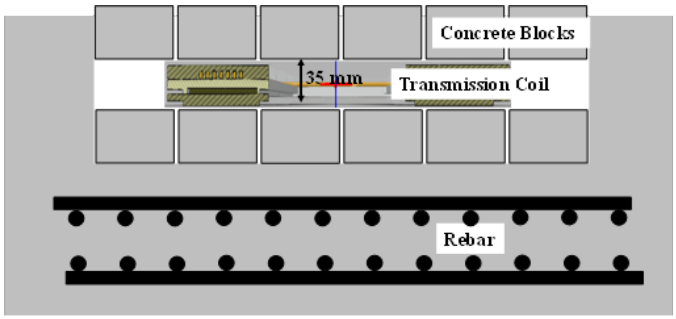

Fig. 3. Schematic diagram of the measurement.

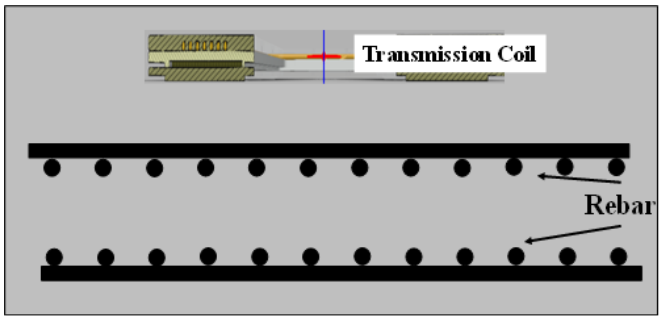

Fig. 4. Completion diagram when put into practical use.

Fig. 5. Normal rebar (Right) and Insulated rebar (Left).

The rebar of the specimen created in this experiment is a double-layered structure with a lattice of rebars as shown in Fig. 1.

The proposed method, insulated rebar, is achieved by wrapping a double layer of soft vinyl chloride tape around the intersection of the rebars. (Fig.5) Measurement with an

Identify applicable funding agency here. If none, delete this text box.

insulation tester (HIOKI 3118) confirmed that insulation was achieved.

III. Concrete Block Burial Simulation Experiment

A. Basic Measurements

The purpose of this experiment is to confirm the electrical characteristics and transmission efficiency of the coil by simulating the conditions of embedding the power transmission coil in reinforced concrete pavement and measuring it.

The equipment used for the measurements was a vector network analyzer (VNA: E5061B), a transmission coil, and a receiving coil (Fig.6).

Table.1 below shows the parameters of the coils used. The number of strands of Litz wire used was 10000, 0.05 mm in strand diameter, and 38 A of allowable current.

The electrical characteristics (coil resistance R [Ω], inductance L [μH], and Q *value*) and transmission characteristics of the transmitting and receiving coils in the pre-embedment were measured using a vector network analyzer (VNA: E5061B). Fig.7 shows the measurement scene, and Table.2 and Table.3 show the results of the VNA measurements.

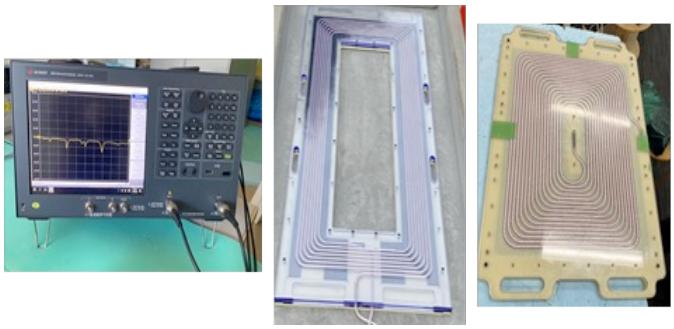

Fig. 6. Measuring instruments.
(Left: VNA, Center: Transmission Coil, Right: Receiver Coil.)

Table. 1. Each parameter of the coils

	Transmission coil	Receiver coil
Coil size	1300×600 mm	580×420 mm
Coil holder size	1600×750×35 mm	800×550×35 mm
Number of turns	7	16
Line pitch	10.85 mm	10.85 mm
Wire diameter	5 mm	5 mm

Fig. 7. Measurements in the pre-embedment.

Table. 2. Electrical characteristics in the air

	Frequency [kHz]	R [Ω]	L [μH]	Q Value
Transmission coil	85	0.056	129.4	1224
Receiver coil	85	0.054	148.1	1454

Table. 3. Transmission characteristics in the air

Frequency [kHz]	Input voltage equivalent [V]	Load [Ω]	Transmission efficiency [%]
85	600	20	95.23

This value will be used to compare and discuss future measurements. For the efficiency measurements, the values in Table.2 were used. The input voltage was set to the 600 V equivalent value and the load was set to maximize the transmission efficiency in the pre-embedment. The resonant frequency was adjusted with a resonant capacitor to 85 kHz before embedment.

B. Measurement of Electrical Characteristics

The concrete blocks and transmission coils were stacked on the test body shown in Fig. 2 to simulate burial in reinforced concrete pavement; Fig. 8 shows a schematic diagram of the measurements. Fig. 9 shows a view of the electrical characteristics measurements.

In Fig.8, The measurement of the five steps:
(i) x=80 mm, y=0 mm (ii) x=60 mm, y=20 mm
(iii) x=40 mm, y=40 mm (iv) x=20 mm, y=60 mm
(v) x=0 mm, y=80 mm
was carried out on two types of test body, one with normal rebar and the other with insulated rebar.

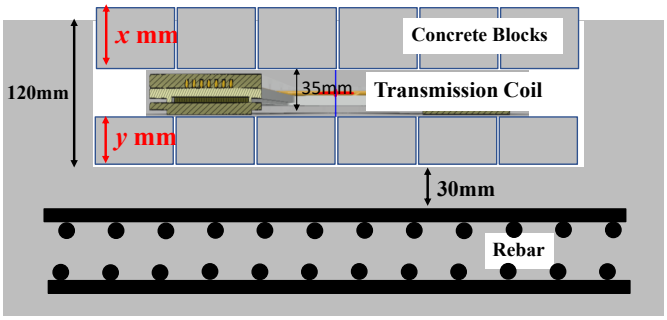

Fig. 8. Schematic of the measurement.

Fig. 9. Status of electrical characteristic evaluation with VNA.

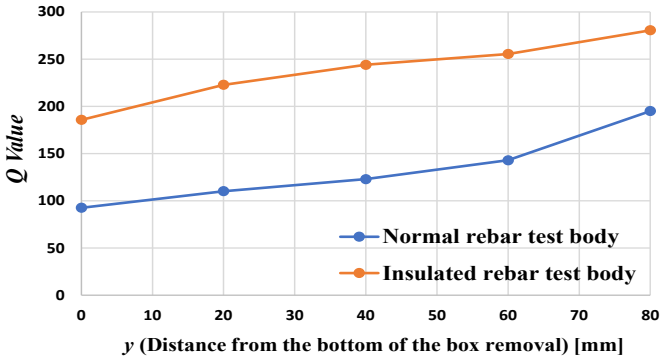

(a) Relation between *y* (distance from the bottom) and *Q*.

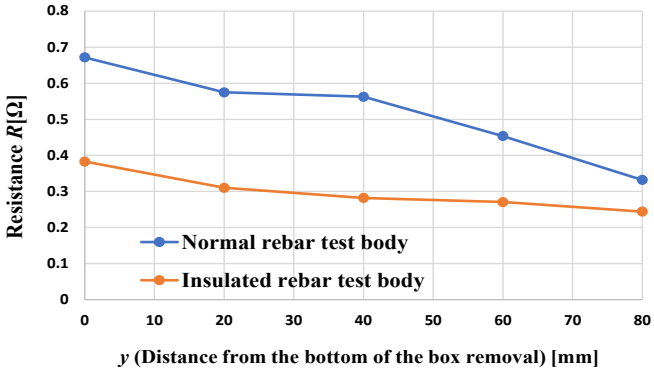

(b) Relation between *y* (distance from the bottom) and *R*.

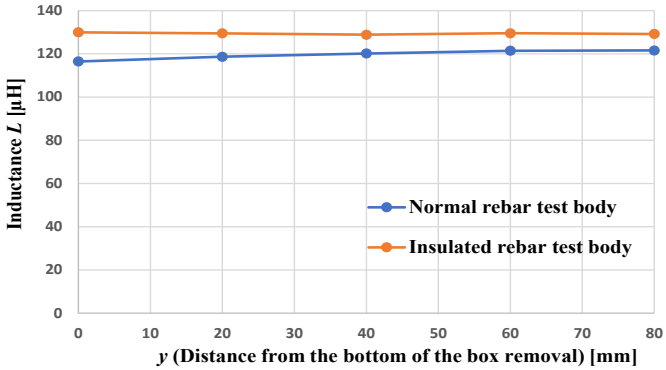

(c)Relation between *y* (distance from the bottom) and *L*.

Fig. 10. Electrical characteristic results.

Fig. 9 shows the measurement view of the electrical characteristics, and Fig. 10 shows the measurement results of the electrical characteristics at VNA.

Fig.10 shows that the resistance and *Q values* of the testbodies before and after embedment were approximately 5.87 and 0.15 times higher, respectively, than those of the conventional rebar, while the resistance and *Q values* of the insulated rebar were approximately 4.32 and 0.22 times higher, respectively, than those of the conventional rebar, confirming the deterioration of properties due to embedment. Furthermore, by using the insulated rebar proposed in this paper, the resistance was successfully reduced to about 0.57 times at y=0 mm and to about 0.74 times at y=80 mm, compared to the case using conventional ordinary rebar. Furthermore, the *Q value* was improved by approximately 50% at y=0 mm and by approximately 30% at y=80 mm, confirming the effectiveness of using insulated steel bars in reducing deterioration of the properties.

In addition, when insulated steel bars were used, the *Q value* was improved by about 34 % by increasing the separation distance from the steel bars by 80 mm, and the reduction effect of property deterioration due to the separation from the steel bars was also confirmed.

C. Measurement of transmission characteristics

Transmission efficiency was also measured; Fig. 11 shows a schematic of the measurements.

In Fig. 9, fixed at *x*=20 mm and the measurement were performed by changing the value of y in 5 steps:
(i) *y*=0 mm (ii) *y*=20 mm (iii) *y*=40 mm (iv) *y*=60 mm
(v) *y*=80 mm
The measurement was performed by changing the value of y in five steps ((i) *y*=0 mm (ii) *y*=20 mm (iii) *y*=40 mm (iv) *y*=60

mm (v) y=80 mm) fixed at x=40 mm and x=60 mm.

Fig. 12 shows the measurement scenery. Fig.13 shows the transmission efficiency by VNA.

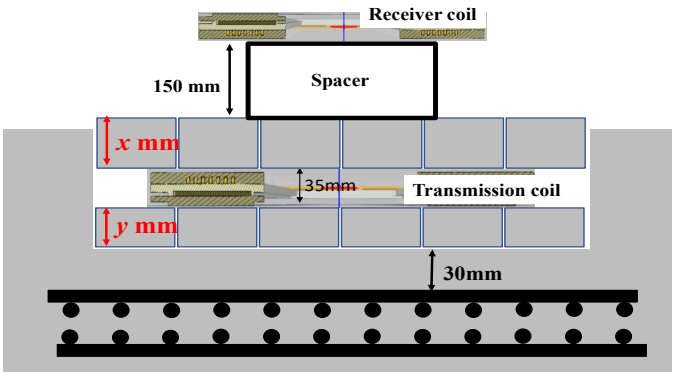

Fig. 11. Schematic of the measurement.

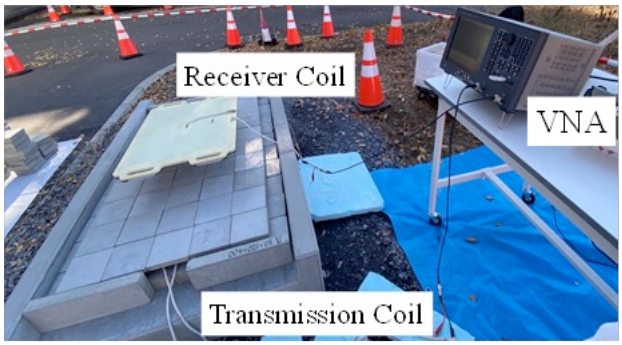

Fig. 12. Status of transmission efficiency evaluation with VNA.

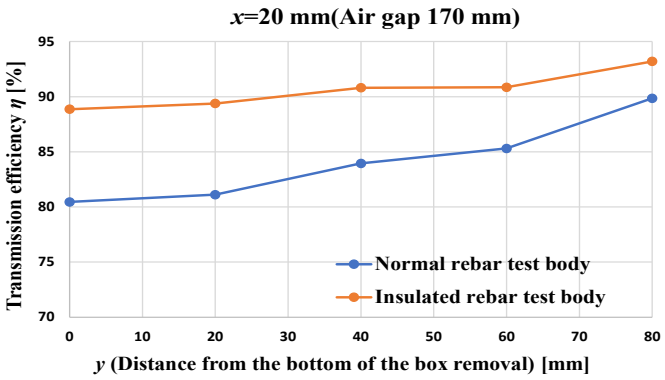

(a) x=20 mm (Air gap 170 mm).

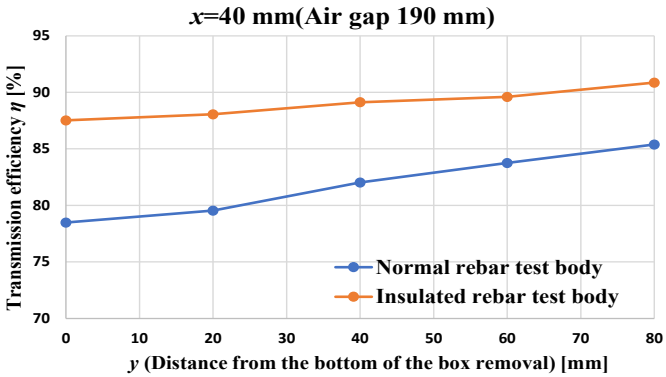

(b) x=40 mm (Air gap 190 mm).

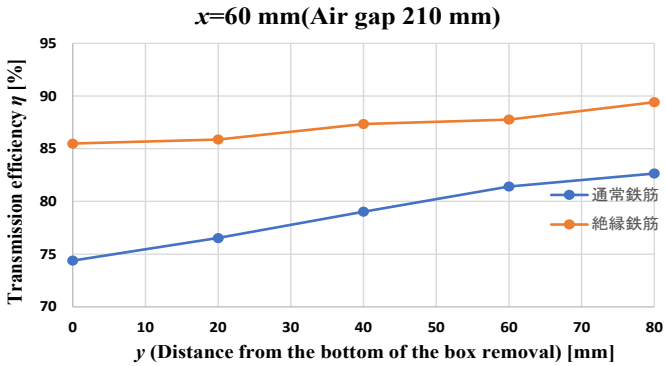

(c) x=60 mm (Air gap 60 mm).

Fig. 13. Transmission efficiency results.

As shown in Fig. 13(a), a maximum transmission efficiency of 93.2 % was obtained, and the transmission efficiency was successfully increased by approximately 3.35 % by using insulated steel bars. Comparing the case when y=0 mm and when y=80 mm, the transmission efficiency increased by approximately 4.34 %, confirming that the transmission efficiency can be increased by increasing the separation distance from the rebar.

In (b), the transmission efficiency decreased by about 2.34 % compared to (a) because the transmission distance increased by 20 mm, resulting in a maximum transmission efficiency of 90.9 %, and the transmission efficiency was successfully increased by about 5.48 % by using insulated rebars.

In case (c), the transmission distance increased by 60 mm compared to case (a), resulting in a decrease of about 3.77 % and a maximum transmission efficiency of 89.5 %, and the transmission efficiency was successfully increased by 6.77 % by using insulated rebars.

Comparing (a), (b), and (c), the transmission efficiency was highest for (a) with the smallest transmission distance of 170 mm. This result was obtained because the lowest ground clearance of the vehicle body was not considered in this

measurement.

IV. Conclusion

In this paper, insulated rebar is proposed as a method to reduce characteristic deterioration in coil embedment in reinforced concrete pavement, and is verified by making measurements on a reinforced concrete test body.

As a result, the use of insulated rebar successfully improved the resistance by a factor of 0.74 and the Q-value by about 30 %. Furthermore, a transmission efficiency of 93.2% was obtained at a transmission distance of 170 mm, and the use of insulated steel bars successfully increased the efficiency by 3.35%.

Future studies will include verification under conditions similar to actual reinforced concrete pavement. In addition, the effects of water, such as rain, and pavement strength will be verified.

References

[1] A. Kurs, A. Karalis, R. Moffatt, J. D. Joannopoulos, P. Fisher, and M. oljacic, “Wireless Power Transfer via trongly Coupled Magnetic Resonances,” cience, Vol. 3 , No. 5834, pp. 83-86, 2007.

[2] G. Covic and J. Boys, “Inductive Power Transfer,” Proceedings of the IEEE, vol. 101, no. 6, pp. 1276-1289, JUN 2013.

[3] Takamitsu Tajima, Hideki Tanaka: “ tudy of 45 -kW Ultra Power Dynamic Charging ystem,” E Technical Paper 8-01-1343 (2018).

[4] B. J. Limb et al., "Economic Viability and Environmental Impact of In-Motion Wireless Power Transfer", IEEE Transactions on Transportation Electrification, vol. 5, no. 1, pp. 135-146, March 2019.

[5] Vincenzo Cirimele, Riccardo Torchio, Antonio Virgillito, Fabio Freschi and Piergiorgio lotto, "Challenges in the Electromagnetic Modeling of Road Embedded Wireless Power Transfer", Energies, vol. 12, pp. 2677, 2019.

[6] H. Fujimoto, O. Shimizu, S. Nagai, T. Fujita, D. Gunji and Y. Ohmori, "Development of Wireless In-wheel Motors for Dynamic Charging: From 2nd to 3rd generation," IEEE PELS Workshop on Emerging Technologies: Wireless Power (WoW), Korea, pp. 56-61, 2020.

[7] A. Torrisi and D. Brunelli, "Magnetic Resonant Coupling Wireless Power Transfer for Lightweight Batteryless UAVs," 2020 International Symposium on Power Electronics, Electrical Drives, Automation and Motion (SPEEDAM), Sorrento, Italy, 2020, pp. 751-756.

[8] Yuto Yamada Takehiro Imura, "An Efficiency Optimization Method of Static Wireless Power Transfer Coreless Coils for Electric Vehicles in the 85 kHz Band Using Numerical Analysis", IEEJ TRANSACTIONS ON ELECTRICAL AND ELECTRONIC ENGINEERING IEEJ Trans 2022, vol.17, Issue 10, pp. 1506-1516, October. 2022.

[9] Yujin Jang, Jung-Kyu Han, Jae-Il Baek, G. -W. Moon, Ji-Min Kim and Hoon Sohn, "Novel multi-coil resonator design for wireless power transfer through reinforced concrete structure with rebar array," 2017 IEEE 3rd International Future Energy Electronics Conference and ECCE Asia (IFEEC 2017 - ECCE Asia), Kaohsiung, Taiwan, 2017, pp. 2238-2243.

[10] Seung-Hwan Lee , Member, IEEE, Myung-Yong Kim, Byung-Song Lee, and Jaehong Lee , Student Member, IEEE, “Impact of Rebar and Concrete on Power Dissipation of Wireless Power Transfer Systems”, IEEE TRANSACTIONS ON INDUSTRIAL ELECTRONICS, VOL. 67, NO. 1, JANUARY 2020,

[11] Benny J. Varghese, Abhilash Kamineni, Nicholas Roberts, Marv Halling,Duleepa J. Thrimawithana and Regan A. Zane ”Design Considerations for 50 kW Dynamic Wireless Charging with Concrete-Embedded Coils”, 2020 IEEE PELS Workshop on Emerging Technologies: Wireless Power Transfer (WoW) November 15 - 19, 2020, Seoul, Korea

[12] S Laporte, G Coquery, V Deniau, A De Bernardinis and N. Hautière, "Dynamic Wireless Power Transfer Charging Infrastructure for Future EVs: From Experimental Track to Real Circulated Roads Demonstrations", World Electric Vehicle Journal, 2019.

[13] K. Hanawa, T. Imura and N. Abe, "Basic Evaluation of Electrical Characteristics of Ferrite-less and Capacitor-less Coils by Road Embedment Experiment for Dynamic Wireless Power Transfer," 2021 IEEE PELS Workshop on Emerging Technologies: Wireless Power Transfer (WoW), San Diego, CA, USA, 2021, pp. 1-5,

[14] K. Hanawa, T. Imura, Y. Hori and N. Abe, "Comparison of Circular Coil, Double-D Coil, and 85 kHz Self-Resonant Coil in Road Embedment for Dynamic Wireless Power Transfer," IECON 2022 – 48th Annual Conference of the IEEE Industrial Electronics Society, Brussels, Belgium, 2022, pp. 1-6

[15] Zhe Feng, Osamu Shimizu, Hayato Sumiya, Sakahisa Nagai, Hiroshi Fujimoto, Masanori Sato,”Influence of Contamination Between Receiver Coil and Embedded Transmitter Coil for Dynamic Wireless Power Transfer System”, 2021 IEEE Workshop on Emerging Technologies: Wireless Power (WoW)

[16] K. Hanawa, T. Imura and N. Abe, "Basic Evaluation of Electrical Characteristics of Ferrite-less and Capacitor-less Coils by Road Embedment Experiment for Dynamic Wireless Power Transfer," 2021 IEEE PELS Workshop on Emerging Technologies: Wireless Power Transfer (WoW), 2021, pp. 1-5

[17] K. M. Koo, S. W. Park, S. H. Park and K. N. Oh, "Diagnosis and Modelling of Equivalent Circuit Combining WPT by Loosely Coupled Coils through CB Concrete Walls at SBO," 2021 International Conference on Advanced Technology of Electrical Engineering and Energy (ATEEE), Qingdao, China, 2021, pp. 51-55.

[18] Z. Wu, M. Chen, X. Duan, Q. Wang, L. Yan and C. Rong, "Analysis of Equivalent Circuit Model of Concrete WPT System," 2022 Asia Power and Electrical Technology Conference (APET), Shanghai, China, 2022, pp. 1-6.